Research Article

For reprint orders, please contact: reprints@future-science.com

Future Medicinal Chemistry

Discovery and biological characterization of a novel scaffold for potent inhibitors of peripheral serotonin synthesis

Nibal Betari*[,1], Kristoffer Sahlholm[2], Yuta Ishizuka[1], Knut Teigen[1] & Jan Haavik[1,3]

[1]Department of Biomedicine, University of Bergen, Jonas Lies vei 91, Postboks 7804, 5020 Bergen, Norway

[2]Department of Integrative Medical Biology, Wallenberg Centre for Molecular Medicine, Umeå University, Johan Bures väg 12, 901 87 Umeå, Sweden

[3]Division of Psychiatry, Haukeland University Hospital, Jonas Lies vei 65, 5021 Bergen, Norway

*Author for correspondence: nibal.betari@uib.no

Aim: Tryptophan hydroxylase 1 (TPH1) catalyzes serotonin synthesis in peripheral tissues. Selective TPH1 inhibitors may be useful for treating disorders related to serotonin dysregulation. **Results & methodology:** Screening using a thermal shift assay for TPH1 binders yielded Compound **1** (2-(4-methylphenyl)-1,2-benzisothiazol-3(2*H*)-one), which showed high potency (50% inhibition at 98 ± 30 nM) and selectivity for inhibiting TPH over related aromatic amino acid hydroxylases in enzyme activity assays. Structure–activity relationships studies revealed several analogs of **1** showing comparable potency. Kinetic studies suggested a noncompetitive mode of action of **1**, with regards to tryptophan and tetrahydrobiopterin. Computational docking studies and live cell assays were also performed. **Conclusion:** This TPH1 inhibitor scaffold may be useful for developing new therapeutics for treating elevated peripheral serotonin.

First draft submitted: 21 April 2020; Accepted for publication: 20 May 2020; Published online: 5 August 2020

Keywords: aromatic amino acid hydroxylases • differential scanning fluorimetry • enzyme inhibitors • kinetics • TPH1 • TPH2 • tryptophan

Serotonin (5-hydroxytryptamine, [5-HT]) is an evolutionarily old monoamine neurotransmitter associated with the control of a broad spectrum of physiological functions in the human body, with important implications for neurology, cardiology and psychiatry [1]. Many different symptoms or disease states have been attributed to decreased or elevated levels of peripheral serotonin, including osteoporosis [2,3], carcinoid syndrome [4,5], obesity and diabetes [6,7], ulcerative colitis [8] and pulmonary arterial hypertension [9,10]. Other research has implicated central serotonin dysregulation in the development of neuropsychiatric disorders; for example, schizophrenia, attention-deficit/hyperactivity disorder (ADHD), anxiety, obsessive-compulsive disorder (OCD) [11] and depression [12,13]. In addition, several studies have indicated elevated levels of serotonin in the blood of children with autism [14,15]. Multiple lines of evidence in animals and patients suggest that modulators of the central and peripheral production of serotonin may prove effective therapeutics for the treatment of these disorders [1,2,13]. TPH exists as two isoforms; TPH1 and TPH2 and catalyzes the initial and rate-limiting step in the biosynthesis of serotonin from the essential amino acid, tryptophan. TPH1 and TPH2 belong to the iron- and pterin-dependent AAAHs. In addition to the TPHs, this family, which shares a highly conserved active site, includes TH and PAH [16,17]. It was long believed that TPH was encoded by a single gene, until Walther *et al.* reported that two distinct genes are responsible for the two TPH isoforms [18,19]. These two isoforms exhibit different patterns of expression, kinetics and regulatory properties [20]. TPH1 is expressed in non-neuronal serotonergic tissues such as enterochromaffin cells of the gut, pancreas, fat, heart and lung, as well as in the pineal gland where it participates in the biosynthesis of melatonin [21–23], while TPH2 is mainly expressed in the central nervous system [24].

Multiple studies have suggested TPH1 as an important drug target for disorders characterized by increased levels of serotonin in peripheral tissues [25,26]. Attempts to develop TPH inhibitors have been undertaken by academia

newlands press

and pharmaceutical companies, (structures of representative TPH1 inhibitors reported in the literature are shown in Supplementary Figure 1), even before the discovery of the second isoform, TPH2. One early TPH inhibitor, p-chlorophenylalanine (pCPA or fenclonine), reached clinical trials ,and was shown to be effective for treating diarrhea in patients with carcinoid syndrome and emesis induced by chemotherapy [27]. However, while pCPA remains a widely used research tool, major side effects, including depression, prevented further clinical development of this compound. The unwanted side effects are likely due to the blood–brain barrier penetration of this compound, effectively reducing CNS serotonin levels, and to the lack of selectivity for the TPH enzymes over the other members of the AAAH family, TH and PAH, with consequent effects on other neurotransmitters [28]. Following the discovery of TPH2, the search has intensified for ligands inhibiting peripheral serotonin synthesis without affecting the CNS. Novel strategies include designing compounds with reduced blood–brain barrier permeability, or allosteric TPH1 inhibitors which bind to less conserved regions out of the active site and therefore may show greater selectivity. A series of compounds; for example, LP-521834, LP-534193 and LP-533401 have been developed by Lexicon Pharmaceuticals (TX, USA), using pCPA as a point of departure [29]. Other spirocyclic, proline-based TPH1 inhibitors, such as KAR5585 and KAR5417, have been developed by Karos Pharmaceuticals (CT, USA) [30]. Both Lexicon and Karos purposely designed these ligands to have low blood–brain barrier permeability. To date, only telotristat ethyl (LX-1032), developed by Lexicon, has been approved by the US FDA for the treatment of carcinoid syndrome-related diarrhea [31,32]. LX-1032 inhibits both TPH1 and TPH2 *in vitro* but selectively lowers 5-HT levels in the GI tract [33]. Most TPH inhibitors have similar affinity for TPH1 and TPH2; however, the pro-drug mol002291, derived from the Chinese herb *Rheum officinalis*, was recently described by Shi *et al.* [34] as a TPH1 inhibitor showing selectivity over TPH2. Finally, a team at Novartis (Basel, Switzerland) recently reported a novel series of allosteric TPH1 inhibitors [35]. However, the similarity of TPH1 and TPH2 to TH and PAH still creates challenges related to specificity since these enzymes share many critical residues in their catalytic sites [36]. Thus, there remains a need for more specific TPH1 inhibitors that do not cross the blood–brain barrier, which could be used to treat disorders associated with peripheral serotonin dysregulation without affecting serotonin levels in the brain. We hypothesized that screening the Prestwick Chemical Library, along with 100 drug-like in-house compounds, might yield TPH1 binders with promising characteristics for further optimization.

Materials & methods

Materials

The Prestwick Chemical Library was purchased from Prestwick Chemical labs (Paris, France). SYPRO Orange was purchased from Sigma-Aldrich (Darmstadt, Germany). Chromatography materials for enzyme purification and the enzymatic activity assays were obtained from Amersham Biosciences (Buckinghamshire, UK) and GE Healthcare, (IL, USA). (6R)-L-erythro-5,6,7,8-tetrahydrobiopterin (BH_4) was from Schircks Laboratories (Bauma, Switzerland), the cytotoxicity LDH Assay Kit was purchased from Tebu-Bio labs (Roskilde, Denmark), while all other reagents, unless otherwise indicated, were obtained from Sigma-Aldrich with a purity of at least 95%. The structures and purities of compounds **1–3** were confirmed by nuclear magnetic resonance (NMR). All NMR spectra were acquired on a 600 MHz Bruker AVANCE NEO NMR Spectrometer (Bruker, MA, USA) using either DMSO-d_6 or HDMSO as the solvent. NMR results are shown in Supplementary Figure 2.

Differential scanning fluorimetry

In order to find TPH1 inhibitors, human doubly truncated TPH1 (ΔNH102–ΔCOOH402) was used for high-throughput screening (HTS) using the differential scanning fluorimetry (DSF) method (a fluorescence-based thermal stability assay) [37,38]. The TPH1 (ΔNH102–ΔCOOH402) coding sequence was cloned into the pET23a vector (6× His C-terminal fusion) between the two sites NdeI and XhoI; and overexpressed in BL21(DE3) *Escherichia coli* cells [39]. After affinity purification and removal of the fusion partner, the proteins were further purified using a Superdex HR 200 column (Amersham) equilibrated with 20 mM Na-HEPES (pH 7.0), 200 mM NaCl as previously described [40].

The Prestwick Chemical Library which consists of 1280 small molecules (95% approved drugs) and 100 in-house small molecules which fulfill the requirements of the Lipinski rule of five were selected and used for DSF screening. The compounds were prepared at a concentration of 10 mM dissolved in 100% DMSO. SYPRO Orange was utilized at 1000× dilution to monitor protein unfolding in a Light Cycler 480 Real-Time PCR System (Roche Applied Science, Penzberg, Germany), using the 384-well format. TPH1 was diluted in 20 mM Na-HEPES (pH 7.0) buffer with 200 mM NaCl, at a final concentration of 0.075 mg/ml. Compounds were added to a final

concentration of 200 μM. Control experiments were performed on each 384-well plate using 2% DMSO in the absence of ligand. The samples were incubated at room temperature for 30 min before measurements were started on the real-time PCR system. The thermal shift curves were recorded in the presence and absence of compounds from 20 to 95°C with four acquisitions per degree centigrade including a 10-s hold at 20°C before and after the experiment.

TPH1 enzymatic activity assay

Enzymatic activity assays were performed with the selected hits from the DSF screening in the presence and absence of 100 μM of each compound. The final concentration of DMSO was 1% (v/v) and control experiments used 1% DMSO in the absence of ligand. TPH1 activities were assayed at 37°C in a standard reaction mixture (100 μl final volume) containing 40 mM Na-HEPES (pH 7.0), 0.05 mg/ml catalase, 10 μM ferrous ammonium sulfate and 20 μM L-tryptophan (L-Trp). The enzymatic reaction was initiated by adding 200 μM BH_4 and 2 mM dithiothreitol (DTT; final concentrations) and stopped by precipitation with 2% (v/v) acetic acid in ethanol. The product, 5-hydroxy-tryptophan (5-OH-Trp), was quantified by high-performance liquid chromatography (HPLC), essentially as described previously by McKinney *et al.* and Winge *et al.* [41], with minor modifications [40,41]. Compounds that reduced TPH1 activity by more than 50% in the preliminary activity assay were selected for further dose-response analyses and IC_{50} determination. The most potent inhibitor from the screening, compound **1**, was selected for further studies.

Structure–activity relationship studies

A structure similarity search of compound **1** was performed using the Zinc database (https://zinc.docking.org) which contains over 230 million purchasable compounds. A total of nine commercially available (in-stock and on-demand) analogs of **1** were selected. The activity assay and IC_{50} determination were performed as described above. Compounds **1–3**, which showed the highest potencies toward TPH1, were selected for further characterization.

Selectivity studies: enzymatic activity assays using other AAAHs

The selectivity of compounds **1–3** for inhibiting TPH1 over the other aromatic amino acid hydroxylases; TPH2, TH and PAH, was evaluated using *in vitro* functional enzyme assays. WT-TPH2 protein was used for this purpose. The proteins were expressed as N-terminal 6 His-MBP fusion proteins, cleaved and purified as described previously [40,41]. The activity assay for TPH2 was performed as described previously by Winge *et al.* [41]. Purified human PAH was expressed and isolated in the *E. coli* strain, BL21-codon plus (DE3) RIL, as described by Flydal *et al.* [42]. The effect of compounds **1–3** on the activity of PAH was evaluated as reported by Aubi *et al.* [43]. Human WT TH was expressed and isolated in *E. coli* BL21(DE3) pLysS, as described previously. Enzyme activity was determined by measuring product formation using HPLC as previously described [44,45].

Mechanism of action & kinetics analysis of compounds 1–3

Mode of inhibition studies were performed for compounds **1–3**, using doubly truncated TPH1 (ΔNH102–ΔCOOH402). The TPH1 activity assay was performed as indicated above in the absence and presence of three different concentrations of each tested compound (0–5 μM). Thus, product formation was measured either at a fixed concentration (200 μM) of the cofactor BH_4 and varying concentrations (0.625–40 μM) of L-tryptophan (L-Trp) or in the presence of varying concentrations of BH_4 (2.4–600 μM) and a fixed concentration (20 μM) of L-Trp. Kinetic parameters were obtained using nonlinear regression to fit the Michaelis–Menten model to the data (see 'Data analysis' section).

Computational studies

Molecular docking was performed with Glide that is part of the Schrödinger program package (Schrödinger Release 2020-1: Glide, Schrödinger LLC, NY, USA). The 'Induced Fit Docking' (IFD) protocol [46] was used to flexibly dock ligands into two defined pockets of TPH1 where sidechains of pocket-residues were re-oriented to accommodate the individual ligands and to optimize calculated interaction energies. TPH1 coordinates used for docking were based on the same construct as used experimentally (Protein Data Bank [PDB] ID: 1MLW) [39]. All water molecules and the cofactor were removed prior to docking. The iron was given a point charge of +2. Two binding pockets were defined for docking; the cofactor pocket, defined by the center of the cofactor in the crystal structure, and the allosteric pocket, where the center of the docking grid box was defined as the center of residues

that form close contacts with allosteric ligands as described by Petrassi *et al.* [35], in other words, residues 190, 280, 283–286, 289, 293, 311–312, 315–316, 321, 330, 354, 376, 378–379, 382 and 386. The grid box dimension was chosen to be big enough to encompass all these residues.

Cell-based enzyme activity assay & cell toxicity

Human embryonic kidney cells (HEK 293FT) were used for the evaluation of cytotoxicity of the compounds. Tested compounds were dissolved in DMSO (final concentration 0.3%) and incubated with the cells for 24 h at concentrations up to 100 μM. Control cells were incubated with 0.3% DMSO in the absence of compounds. After 24 h incubation, the effects of cytotoxicity were determined using a standard LDH assay, as described by the manufacturer (Tebu-bio).

The cell-based enzyme activity assay was carried out using HEK 293FT cells transiently transfected with full-length *hTPH1* in pcDNA 3.1 (Genscript, NJ, USA). The transfection was performed using lipofectamine (Gibco, MD, USA) according to the manufacturer's instructions. Cells were incubated in 24-well plates coated with poly-D-lysine. After 24h incubation, the cells were harvested, lysed and centrifuged (16,000×*g* at 4°C for 10 min) essentially as described by Winge *et al.* [41], and the extracted 5-OH-Trp was measured using HPLC–fluorometric detection as described above.

Data analysis

Effects of compounds on the thermal stability of the enzyme were determined as a change in the melting temperature, T_m ($\Delta T_m = T_m - T_{m,ref}$) in the presence of 200 μM of the compound. $T_{m,ref}$ is defined as the control melting temperature in the presence of 2 % DMSO. GraphPad Prism Version 8 (CA, USA) was used for the analysis of enzyme inhibition data. IC_{50} values were calculated using nonlinear regression, fitting the following Equation (1) to the data:

$$Y = \text{bottom} + (\text{Top} - \text{Bottom}) / (1 + 10^{(X - \log IC50)}) \quad \text{(Eq. 1)}$$

where Y is the response as a fraction of 1, X is the logarithm of ligand concentration, Top is the maximum response and bottom is the minimum response in the presence of ligand. For estimation of kinetic parameters, fitting of the Michaelis–Menten equation (Equation 2) to data yielded V_{max} and K_M.

$$Y = V_{max} \times X / (K_M + X) \quad \text{(Eq. 2)}$$

where X is the substrate concentration and Y is enzyme velocity. *In vitro* assay and cell data are presented as mean ± standard deviation (SD).

Results & discussion

Identification of potential TPH1 inhibitors using DSF

To identify novel ligands with TPH1-modifying activity, HTS using DSF detection was performed using a commercial screening library (Prestwick 1280) and 100 in-house molecules. The shift in the midpoint denaturation temperature ΔT_m was recorded to find binders that could alter the thermodynamic stability of TPH1. The fluorescent dye, SYPRO Orange, was used to record the T_m of the protein. Hits were identified by determination of ΔT_m ($\Delta T_m = T_m - T_{m,ref}$). The mean control value ($T_{m,ref}$) in the presence of 2% DMSO was 51.8 ± 0.47°C. Compounds which induced a positive thermal shift were considered stabilizers and compounds which caused a negative thermal shift were considered destabilizers. A total of 90 compounds were selected as preliminary hits (Figure 1). Whereas the utility of DSF destabilizers has been debated, recent studies have revealed that such compounds might often represent useful hits [47,48]. Thus, 40 compounds that stabilized TPH1 with $\Delta T_m \geq 3$°C or destabilized the protein with $\Delta T_m \leq -3$°C were selected among the preliminary hits for further investigation. These compounds were subsequently subjected to further validation and investigation in concentration–response DSF experiments, followed by an enzyme activity assay using HPLC with fluorometric detection to quantify 5-OH-Trp.

Preliminary hits from the DSF screen, which showed at least 50% inhibitory activity at 100 μM in the enzyme activity assay, were identified as primary hits and subjected to further analyses and determination of IC_{50} values. The top candidate, compound **1** (2-(4-methylphenyl)-1,2-benzisothiazol-3 (2*H*)-one), also known as PBIT, reduced the activity of hTPH1(ΔNH102–ΔCOOH402) with nanomolar potency (IC_{50} = 0.098 ± 0.030 μM; Figure 2B). Whereas truncated TPH1 was used for DSF screening and further characterization in the enzyme assay, **1** showed

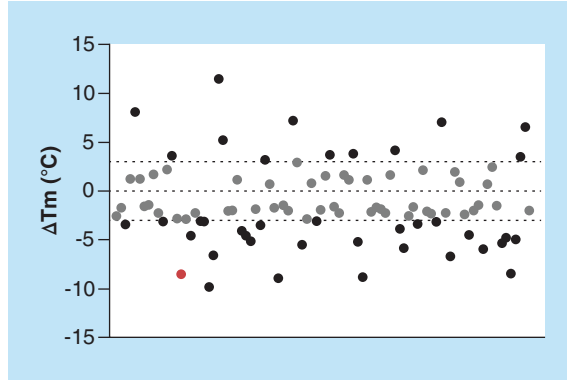

Figure 1. Results of high-throughput screening using differential shift fluorimetry to identify binders to TPH1. Human doubly truncated TPH1 (ΔNH102–ΔCOOH402) was used for screening. Compounds that showed ΔT_m between -3 and +3°C are shown as gray dots, while compounds inducing positive or negative ΔT_m changes of 3°C or greater are shown as black dots. These 40 hits underwent further characterization. Compound **1** (2-(4-methylphenyl)-1,2-benzisothiazol-3(2*H*)-one) is shown as a red dot and destabilized TPH1, resulting in ΔT_m = -8.5°C. Dotted horizontal lines indicate ΔT_m -3, 0 and 3°C.

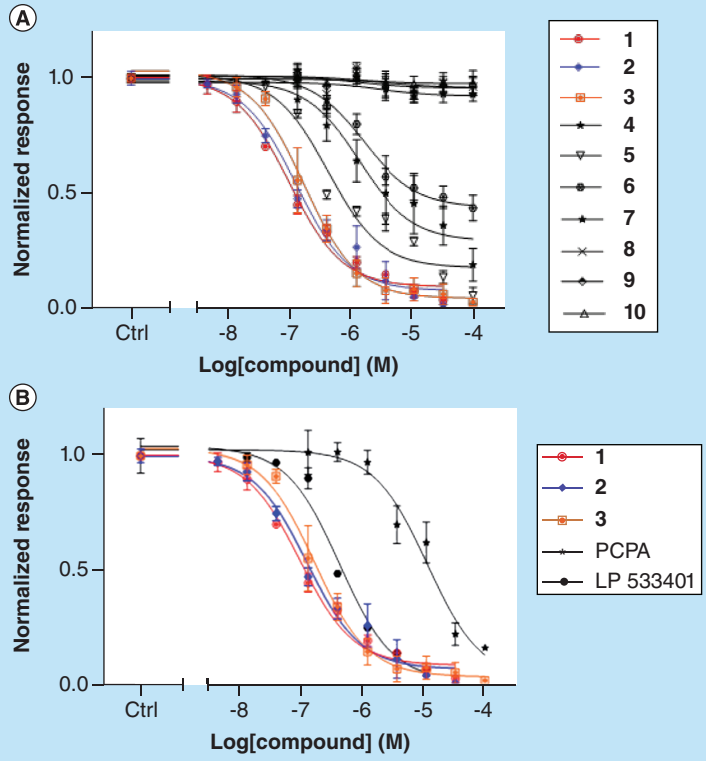

Figure 2. Results of structure–activity relationship studies. (A) Effect of the analogs of **1** tested against TPH1. **(B)** Comparison of the inhibitory activities of **1–3** with the reference compounds, pCPA and LP 533401, at TPH1. Human doubly truncated TPH1 (ΔNH102–ΔCOOH402) was used in these studies. Data represent means ± standard deviation of three separate experiments performed in duplicate.
Ctrl: Control; pCPA: p-Chlorophenylalanine.

very similar inhibitory activity at full-length TPH1 (IC_{50} = 0.096 ± 0.057 μM; Supplementary Figure 3). Thus, **1** was found to be more potent than the commercially available TPH1 inhibitor reference compounds; in our assay, pCPA displayed an IC_{50} of 11.250 ± 0.097 μM, whereas LP 533401 showed an IC_{50} of 0.409 ± 0.060 μM (Figure 2B & Table 1). Sayegh *et al.* previously reported that **1** inhibits the histone demethylase JARID1B *in vitro* with an IC_{50} of 3 μM [49].

A compound similarity search of the ZINC database was performed with the aim of studying the structure–activity relationships (SAR) of compounds related to **1** as TPH1 inhibitors. Nine analogs of **1** were identified and purchased; structures of the compounds are shown in (Table 1). Interestingly, three of these compounds; **2**, **3** and **4**, showed relatively high potency in inhibiting TPH1 activity, while compound **5**, which contains a secondary-

Table 1. Inhibitory activities of reference compounds, pCPA and LP533401, compound 1 and selected analogs of compound1 at human doubly truncated TPH1 (Δ NH102–Δ COOH402).

Name	Structure	IC_{50} (μM)
pCPA	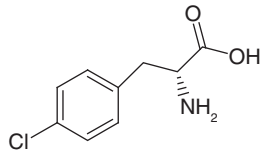	11.250 ± 0.097
LP-533401	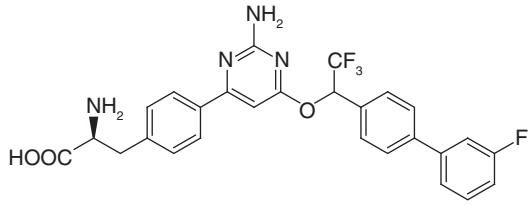	0.409 ± 0.060
Compound **1** (2-(4-methylphenyl)-1,2-benzisothiazol-3(2*H*)-one)	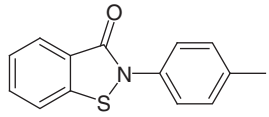	0.098 ± 0.030
Compound **2** (2-phenylbenzo[d]isothiazol-3(2*H*)-one)	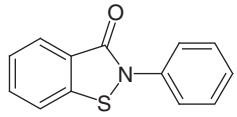	0.129 ± 0.044
Compound **3** (2-(thiazol-2-yl) benzo [d]isothiazol-3(2*H*)-one)	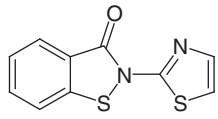	0.170 ± 0.046
Compound **4** (2-phenylisothiazol-3(2*H*)-one)	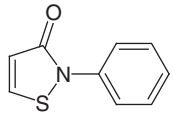	0.419 ± 0.069
Compound **5** (benzo[d]isothiazol-3(2*H*)-one)	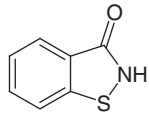	1.367 ± 0.092
Compound **6** (2-(4-(piperidin-1-ylsulfonyl)phenyl)benzo [d]isothiazol-3(2*H*)-one)	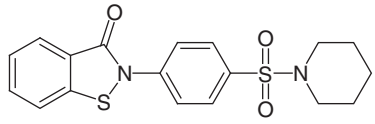	1.616 ± 0.061
Compound **7** (2-phenylbenzo[d]isox, azol-3(2*H*)-one)	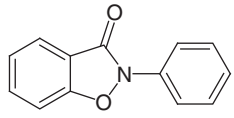	>100
Compound **8** (2-phenyl-1,2-dihydro-3*H*-indazol-3-one)	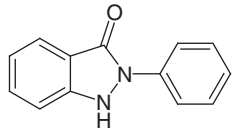	>100

IC_{50} (μM) values are shown for the compounds which showed inhibitory activity. Data are mean ± standard deviation from three independent experiments, each performed in duplicate.
IC_{50}: Half maximal inhibitory concentration.

Table 1. Inhibitory activities of reference compounds, pCPA and LP533401, compound 1 and selected analogs of compound1 at human doubly truncated TPH1 (Δ NH102–Δ COOH402) (cont.).

Name	Structure	IC_{50} (μM)
Compound **9** (2-phenylbenzo[b]thiophen-3(2*H*)-one)	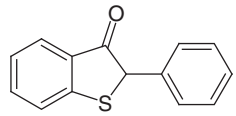	>100
Compound **10** (2-phenylbenzo[d][1,2] selenazol-3(2*H*)-one)	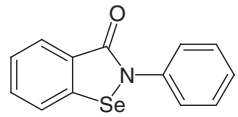	>100

IC_{50} (μM) values are shown for the compounds which showed inhibitory activity. Data are mean ± standard deviation from three independent experiments, each performed in duplicate.
IC_{50}: Half maximal inhibitory concentration.

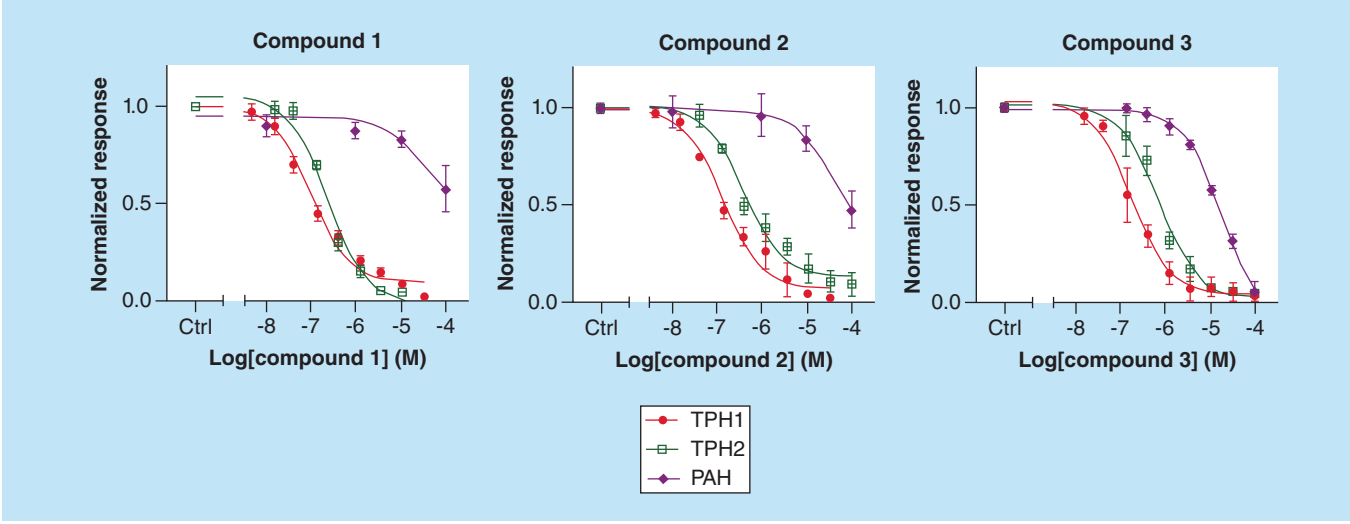

Figure 3. Selectivity of 1–3 at AAAH. *In vitro* enzyme activity assays were used to evaluate the selectivity of the most potent compounds, **1–3**, to inhibit TPH1 and the other aromatic amino acid hydroxylases; TPH2, TH (not shown) and PAH. Human doubly truncated TPH1 (ΔNH102–ΔCOOH402) was used in these studies, whereas the other enzymes were full length. Data represent means ± standard deviation of three separate experiments performed in duplicate.

instead of a primary amine in the isothiazol moiety, showed considerably less potent inhibitory activity. The larger molecule, compound **6** showed weak inhibitory activity as well. Compounds **7**, **8**, **9** and **10** did not show any inhibition of TPH1 in the activity assay at concentrations up to 100 μM. Clearly, the isothiazol moiety appears to be key for the inhibitory activity, as replacement of its sulfur atom with oxygen (compound **7**), nitrogen (compound **8**), or selenium (compound **10**) led to a loss of activity. Replacement of the isothiazol ring with a thiophene ring (compound **9**) also resulted in a loss of TPH1 inhibitory activity. The SAR results are summarized in Figure 2A and Table 1. Compounds **1**, **2** and **3**, which showed the highest potency to inhibit TPH1 (Figure 2B), were selected for further study using Michaelis–Menten kinetic analyses and computational docking.

Since the active site is highly conserved among the AAAHs, selectivity is a challenge when attempting to develop putative therapeutic ligands for any one of these enzymes. Although the 3D crystal structures of these hydroxylases have provided a better understanding of the relatively minor differences that do exist between their active sites, developing selective ligands for each of these hydroxylases remains a difficult task to this day [36,50,51]. Therefore, it was relevant to determine the inhibitory potencies of **1–3** at each of the AAAHs. *In vitro* activity assays revealed that **1–3** inhibited TPH2 with similar potency as TPH1, being two- to fourfold more potent at the latter enzyme, while **1** and **2** inhibited PAH with at least 200-fold lower potency, compared with TPH1 (Figure 3 & Table 2). **3** showed 100-fold lower potency at PAH, relative to TPH1. Interestingly, none of the compounds produced any appreciable inhibition of TH, even at 100 μM (not shown). Thus, this new scaffold can be considered selective

Table 2. Selectivity of 1–3 at enzymes of the AAAH family.

Enzyme name	Compound 1 IC_{50} (μM)	Compound 2 IC_{50} (μM)	Compound 3 IC_{50} (μM)
hTPH1	0.098 ± 0.030	0.129 ± 0.044	0.171 ± 0.046
hTPH2	0.229 ± 0.040	0.383 ± 0.051	0.708 ± 0.044
hPAH	>25	>25	18.64 ± 0.030
hTH	>100	>100	>100

The data are expressed as means ± standard deviation from three independent experiments, each performed in duplicate.
IC_{50}: Half maximal inhibitory concentration.

Table 3. Enzyme kinetic parameters of TPH1 in the absence and presence of the tested compounds.

Substrate, concentration	Inhibitor concentration (μM)	Compound 1		Compound 2		Compound 3	
		V_{max} (nmol/min/mg)	K_M (μM)	V_{max} (nmol/min/mg)	K_M (μM)	V_{max} (nmol/min/mg)	K_M (μM)
L-Trp† 0.625–40 μM BH_4 200 μM	0	42.66 (40.58–44.87)	3.82 (3.2–4.53)	42.66 (40.58–44.87)	3.82 (3.21–4.53)	42.66 (40.58–44.87)	3.82 (3.2–4.53)
	0.05	24.60 (22.78–26.59)	2.84 (2.1–3.78)	26.75 (25.12–28.50)	3.04 (2.41–3.83)	42.33 (40.37–44.41)	3.97 (3.38–4.66)
	0.5	19.02 (16.40–22.51)	9.9 (6.63–15.2)	11.08 (10.28–11.95)	3.10 (2.36–4.06)	22.26 (20.92–23.75)	9.31 (7.87–11.04)
	5	4.12 (3.87–4.40)	5 (4.1–6.1)	4.01 (3.70–4.35)	2.26 (1.65–3.07)	4.752 (4.180–5.46)	7.33 (5.03–10.7)
BH4‡ 2.4–600 μM L-Trp 20 μM	0	58.69 (57.03–60.39)	22.47 (19.9–25.25)	58.69 (57.03–60.39)	22.47 (19.9–25.25)	58.69 (57.03–60.39)	22.47 (19.9–25.25)
	0.05	45.79 (43.47–48.20)	19.10 (15.3–23.69)	52.00 (49.23–54.87)	19.3 (15.43–24.03)	55.46 (53.58–57.38)	21.34 (8.53–24.54)
	0.5	27.15 (26.48–27.83)	14.06 (12.57–15.72)	20.53 (19.97–21.10)	21.11 (18.75–23.70)	24.87 (23.87–25.90)	30.15 (25.66–35.38)
	5	9.39 (8.89–9.92)	17.86 (13.99–22.72)	7.62 (7.01–8.35)	20.1 (13.40–29.95)	9.465 (8.67–10.33)	30.95 (21.44–44.41)

†Kinetic measurements at a fixed concentration of BH_4 and varying concentrations of L-Trp.
‡Kinetic measurements at a fixed concentration of L-Trp and varying concentrations of BH_4. Values in brackets represent 95% CI of the fit of the Michaelis–Menten equation to data. Data represent means of two separate experiments performed in duplicate.
K_M: Michaelis–Menten constant; V_{max}: Maximum rate of reaction.

for TPH1 and TPH2 over PAH and TH. Further characterization of the binding mode of these inhibitors may provide useful insights for the future development of more selective AAAH inhibitors.

Kinetic characterization of TPH1 inhibition by 1–3

Human doubly truncated TPH1 (ΔNH102–ΔCOOH402) was used for kinetic protein–ligand interaction studies. Enzyme assays were conducted as described previously. The mechanisms of action of **1–3** at TPH1 were investigated by measuring enzyme inhibition at different concentrations of inhibitor, amino acid substrate, and tetrahydrobiopterin (BH_4) cofactor. Kinetic parameters for both L-Trp and BH_4 were calculated by fitting the Michaelis–Menten equation to the data using nonlinear regression, in the absence and presence of different concentrations of **1–3** (0–5) μM. When the kinetics of the compounds were measured at different concentrations of the substrate L-Trp (0.625–40) μM, the concentration of the cofactor, BH_4, was fixed at 200 μM. As shown in Table 3, there was a progressive decrease in V_{max} while K_M remained virtually unchanged with increasing inhibitor concentration. Similarly, when the concentration of the co-factor, BH_4, was varied (2.4–600 μM), in the presence of a fixed concentration of L-Trp (20 μM), a decrease in V_{max} and a nearly constant K_M was again observed with increasing concentrations of the three compounds (Table 3). These results indicate that **1–3** are noncompetitive inhibitors, both with respect to tryptophan and to the co-factor, BH_4. Steady-state inhibition data of **1–3** for TPH1 are shown in Figure 4.

Previous studies revealed that all four AAAH enzymes can use any of the three aromatic amino acids as substrate [36]. Thus, for example, PAH may be a source of 5-HT *in vivo* since this enzyme is able to catalyze the hydroxylation of L-Trp to 5-OH-Trp *in vitro* [52]. In addition, these enzymes use the same pterin co-factor to convert the iron in their active sites to the ferrous form, which is a key step in the catalysis of the hydroxylation

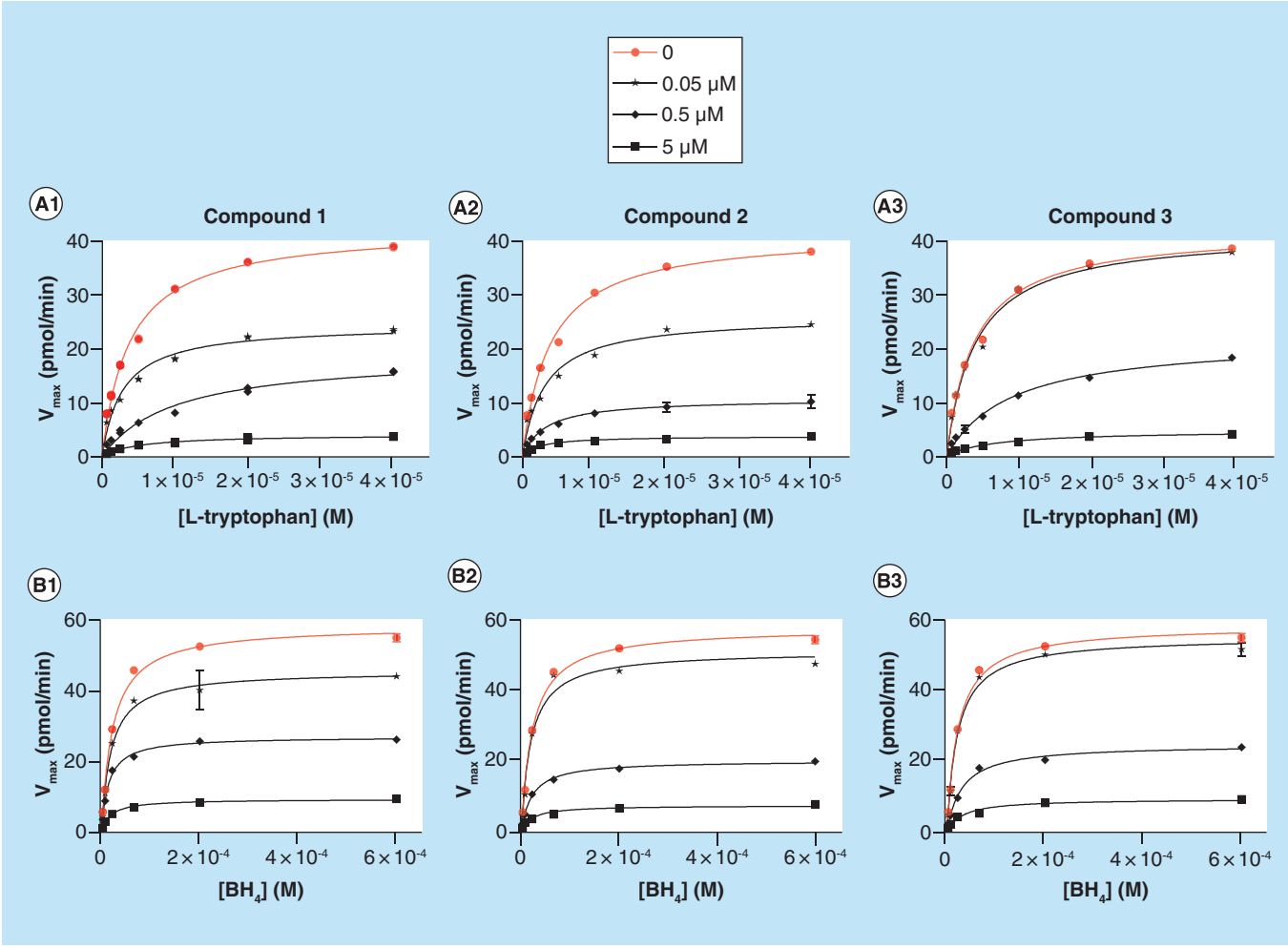

Figure 4. Mechanism of TPH1 inhibition by 1–3. Kinetic study of TPH1 inhibition by **1–3** in the presence of varying concentrations of substrate (L-tryptophan, panels **A1–A3**) or cofactor (BH_4, panels **B1–B3**). The Michaelis–Menten equation was fitted to data using nonlinear regression. The data reveal a decrease in the V_{max} value with increasing concentration of the compound, while K_M is not appreciably affected. Thus, **1–3** appear to inhibit TPH1 a noncompetitive manner with regard to both L-Trp and BH_4.

reaction [36,53]. However, finding ligands which can inhibit TPH1 in a noncompetitive fashion, with respect to both the substrate and the co-factor, may be a promising strategy for the development of therapeutic ligands which selectively inhibit TPH1, as such ligands would be expected to bind outside the conserved active site. TPH1 inhibitors with potency in the low nanomolar range have been reported by Lexicon Pharmaceuticals [54–56]. These compounds, however, were derived from pCPA and based on a phenylalanine moiety. As could be expected, they were found to behave competitively with regards to the substrate [29].

Computational studies

Computational docking studies were performed to explore how the compounds might interact with TPH1. **1–3** were docked to the cofactor binding site and the allosteric site of TPH1 (as defined in the 'Materials & methods' section). Table 4 shows the estimated free energies of binding for the three compounds to each of the two pockets.

1 had the strongest predicted binding affinity to the cofactor site, with a docking score of -10,53, whereas **2** and **3** were estimated to have slightly lower binding affinities. A closer look at the docked complexes (Supplementary Figure 4) revealed that the carboxyl group of **1** positioned in close proximity to the active site iron, with the benzothiazol rings sandwiched between Phe 241 and Tyr 235, similar to what is observed for BH_4 in the crystal structure, where the carbonyl group of BH_4 is oriented toward the active site iron and the pteridine rings are stacked between Phe 241 and Tyr 235. In addition, the sulfur atom of **1** had the possibility of making S–π interactions

Table 4. Docking scores and estimated dissociation constants of compounds docked in the cofactor and allosteric pockets of TPH1.

	Cofactor pocket		Allosteric pocket	
	Docking score	Calculated K_d† (μM)	Docking Score	Calculated K_d† (μM)
Compound **1**	-10.53	0.02	-8.51	0.58
Compound **2**	-9.70	0.08	-8.84	0.33
Compound **3**	-9.04	0.23	-8.18	1.00

Docking scores were calculated using the scoring function in the Glide software on individual docked complexes to approximate the free energies of binding, where a more negative score indicates more favorable interactions.
†The K_d in the table are calculated from the docking score, as a crude approximation to experimental K_d values.
K_d: Dissociation constants.

with Phe 241 and Tyr 235 while the toluene ring was involved in anion–π interactions with Glu 317. The toluene methyl group filled a hydrophobic void defined by Ile 366, Phe 318, and Cys 364. **2** docked similarly to **1** to the cofactor binding site, without filling the hydrophobic void due to the lack of a methyl group, which might explain the slightly lower estimated binding affinity of **2** versus **1**. **3** was also sandwiched between Phe 241 and Tyr 235, with its carbonyl oxygen oriented toward the active site iron and the thiazole ring involved in anion-π interactions with Glu 317. The predicted binding affinity of **3** is lower than for **1** and **2**.

1–3 were also docked to the postulated allosteric binding site of TPH1 (Supplementary Figure 4). **1** was found to stack the benzothiazol rings in between two aromatic residues, Phe 330 and 379, with possible S–π and π–π interactions. The carbonyl group of **1** had the possibility to make hydrogen bond interactions with the backbone of Ser 378 and side chain of Ser 376. The toluene group was near both Phe 289 and Phe 286, with the possibility of π–π interactions. **2** and **3** interacted in a similar way, with stacking interactions involving the same residues of the allosteric site.

It should be noted that the allosteric site is a much more challenging pocket to dock compounds into as compared with the cofactor site. The crystal structure used in this study is that of TPH1 in complex with a cofactor analog. Thus, when the cofactor is removed prior to docking, the cofactor binding pocket is preformed to accommodate ligands. This is not the case for the postulated allosteric site, where an induced conformational change is assumed to take place upon binding of ligands. Although the induced fit docking protocol was used here, it may well be that the allosteric binding pocket is more flexible to accommodate ligands than the protocol can account for. Thus, the predicted binding poses and docking scores are less reliable for this pocket. The inability to fully account for conformational changes penalizes size of the docked ligand, as a bulkier ligand would need more space and more flexibility of the receptor to be accommodated. Thus, we would expect that the predicted binding affinities for the allosteric site are underestimated and that **1** is penalized the most due to it being the bulkiest of the three compounds.

Cell-based assay assessment

Cell toxicity assessment of 1

1, revealed to be the most potent inhibitor in this study, was subjected to cell toxicity assessment and a cell-based TPH1 inhibition assay. Cell toxicity was determined using the HEK 293FT cell line. The cells were incubated with different concentrations of the tested compounds; **1** and the reference TPH1 inhibitor, LP-533401, and their cytotoxicity was evaluated by measuring the liberation of LDH into the surrounding medium. The results shown in Supplementary Figure 5 indicate that **1** did not show significant cytotoxicity at 3.3 μM, although there was a trend toward significance at concentrations of 10 and 30 μM.

Cell-based TPH1 inhibition assay

A cell-based assay using HEK 293FT cells transiently transfected with TPH1 was employed to determine intracellular TPH1 inhibition. Cells were incubated with test compound, or vehicle, for 24 h prior to measuring the synthesized 5-OH-Trp using HPLC–fluorometric detection. **1** showed inhibition 5-OH-Trp synthesis with an IC_{50} of 0.528 ± 0.25 μM, while LP533401 displayed an IC_{50} of 0.955 ± 0.106 μM (data not shown). These results indicate that **1** exhibits a sufficient degree of cell penetration to be able to inhibit TPH1 in cultured cells.

Conclusion

In summary, via high-throughput screening using the DSF technique and medium-throughput screening using a functional enzyme assay, we discovered a promising new scaffold for TPH1 inhibitors. Several compounds sharing this scaffold inhibited TPH1 with nanomolar affinity. Compared with previously reported inhibitors, our new compounds were more selective toward TPH over the other aromatic amino acid hydroxylases, TH and PAH. Preliminary docking studies revealed that the compounds can be accommodated in both the cofactor- and the allosteric binding site of TPH1, contacting aromatic residues in both sites mainly through stacking interactions. Kinetic characterization of **1–3** suggests that they are noncompetitive toward both the cofactor and the substrate, indicating that they may not bind to the cofactor binding site. Instead, these compounds may elicit their inhibitory effects through allosteric interactions, either via the previously identified allosteric site, or by binding elsewhere in the protein. Cell-based evaluations revealed **1** to display low toxicity and good ability to penetrate cell membranes. We envisage that this series of compounds may be useful leads for developing new therapeutics for the treatment of disorders related to dysregulation of peripheral serotonin.

Future perspective

The discovery of inhibitors of serotonin synthesis directly acting on the two isoforms of tryptophan hydroxylase is an attractive aim for academia and pharmaceutical industry. For example, selective TPH1 inhibitors may address previously unmet clinical needs by correcting disorders related to dysregulation of peripheral serotonin. A number of TPH1 inhibitors have already been described; most of these have been developed to have TPH1 inhibitory activity limited to the gut. Hitherto, only one such compound has been approved by the FDA for the treatment of carcinoid syndrome-related diarrhea. Our effort to find new TPH inhibitors led to the identification of three compounds sharing a new scaffold, which may exert their inhibition by binding to a region outside the catalytic site. Thus, this novel scaffold can potentially be exploited for further development of inhibitors showing greater selectivity over the other AAAHs, including TPH2, and a more favorable side effect profile compared with presently available TPH inhibitors. This biological profile warrants further study (e.g., co-crystallization and *in vivo* evaluation) to assess their mechanism of action and potential as peripheral serotonin inhibitor drug candidates. A limitation of this study is that compounds **1–3** inhibit TPH1 and TPH2 with similar potencies. It will therefore be important to further investigate their blood–brain barrier permeability, as well as their uptake and effect on serotonin concentrations in peripheral and brain tissues, to assess whether they might selectively target TPH1 *in vivo* due to low brain penetration. Finally, it will be relevant to determine whether the noncompetitive nature of TPH1 inhibition observed in the present investigation reflects irreversible binding of compounds **1–3** to TPH1. For a peripherally-acting compound, such an irreversible action may be clinically favorable, as it would prolong the effect of a single drug dose. This in turn might enable reduced dosage, lower off-target drug exposure and hence reduced side effect liability.

Summary points

- Tryptophan hydroxylase catalyzes the synthesis of serotonin and belongs to the family of aromatic amino acid hydroxylases which shares a similar catalytic domain.
- Both academia and the pharmaceutical industry have taken an interest in developing TPH1 inhibitors for treating disorders related to dysregulation of peripheral serotonin.
- Several TPH1 inhibitors have been reported, but only one has been approved by the US FDA.
- Differential shift fluorimetry represents a successful high-throughput screening method for finding small-molecule ligands of TPH1.
- Here, we present compounds sharing a new scaffold and which showed nanomolar potency in inhibiting TPH1 and selectivity over the other aromatic amino acid hydroxylases, phenylalanine hydroxylase and tyrosine hydroxylase.
- Docking studies suggest the compounds can be accommodated in both the cofactor and allosteric site where they bind mainly through stacking interactions.
- The most promising inhibitor, compound **1**, demonstrated low toxicity and ability to cross the cell membrane of HEK 239FT cells.
- The new scaffold represents a promising lead for developing new therapeutic agents for disorders related to the dysregulation of serotonin synthesis.

Supplementary data

To view the supplementary data that accompany this paper please visit the journal website at: www.future-science.com/doi/suppl/10.4155/fmc-2020-0127

Acknowledgments

The authors would like to thanks A Martinez and her group for providing the PAH and TH enzymes. E Hausvik is thanked for his help and technical support. J Underhaug is acknowledged for the NMR analysis. Molecular docking was performed on resources provided by UNINETT Sigma2 – the National Infrastructure for High-Performance Computing and Data Storage in Norway.

Financial & competing interests disclosure

This study was financed by the European Union's Horizon 2020 research and innovation program under grant agreement no. 667302 (CoCA) and Stiftelsen K. G. Jebsen (SKGJ-MED02). This work was partly supported by the Bergen Research Foundation, Sparebankstiftinga Sogn og Fjordane and the Research Council of Norway through the Norwegian NMR Platform (NNP) (226244/F50). The authors have no other relevant affiliations or financial involvement with any organization or entity with a financial interest in or financial conflict with the subject matter or materials discussed in the manuscript apart from those disclosed.

No writing assistance was utilized in the production of this manuscript.

References

1. Matthes S, Bader M. Peripheral serotonin synthesis as a new drug target. *Trends Pharmacol. Sci.* 39(6), 560–572 (2018).
2. Yadav VK, Balaji S, Suresh PS *et al.* Pharmacological inhibition of gut-derived serotonin synthesis is a potential bone anabolic treatment for osteoporosis. *Nat. Med.* 16(3), 308–312 (2010).
3. Inose H, Zhou B, Yadav VK, Guo XE, Karsenty G, Ducy P. Efficacy of serotonin inhibition in mouse models of bone loss. *J. Bone Miner. Res.* 26(9), 2002–2011 (2011).
4. Hallen A. Fibrosis in the carcinoid syndrome. *Lancet* 1(7336), 746–747 (1964).
5. MacDonald RA, Robbins SL, Mallory GK. Dermal fibrosis following subcutaneous injections of serotonin creatinine sulphate. *Proc. Soc. Exp. Biol. Med.* 97(2), 334–337 (1958).
6. Crane JD, Palanivel R, Mottillo EP *et al.* Inhibiting peripheral serotonin synthesis reduces obesity and metabolic dysfunction by promoting brown adipose tissue thermogenesis. *Nat. Med.* 21(2), 166–172 (2015).
7. Oh CM, Namkung J, Go Y *et al.* Regulation of systemic energy homeostasis by serotonin in adipose tissues. *Nat. Commun.* 6, 6794 (2015).
8. Margolis KG, Stevanovic K, Li Z *et al.* Pharmacological reduction of mucosal but not neuronal serotonin opposes inflammation in mouse intestine. *Gut* 63(6), 928–937 (2014).
9. Dempsie Y, Morecroft I, Welsh DJ *et al.* Converging evidence in support of the serotonin hypothesis of dexfenfluramine-induced pulmonary hypertension with novel transgenic mice. *Circulation* 117(22), 2928–2937 (2008).
10. Morecroft I, Dempsie Y, Bader M *et al.* Effect of tryptophan hydroxylase 1 deficiency on the development of hypoxia-induced pulmonary hypertension. *Hypertension* 49(1), 232–236 (2007).
11. Jacobsen KK, Kleppe R, Johansson S, Zayats T, Haavik J. Epistatic and gene wide effects in YWHA and aromatic amino hydroxylase genes across ADHD and other common neuropsychiatric disorders: association with YWHAE. *Am. J. Med. Genet. B Neuropsychiatr. Genet.* 168(6), 423–432 (2015).
12. Zhang X, Gainetdinov RR, Beaulieu JM *et al.* Loss-of-function mutation in tryptophan hydroxylase-2 identified in unipolar major depression. *Neuron* 45(1), 11–16 (2005).
13. Matthes S, Mosienko V, Bashammakh S, Alenina N, Bader M. Tryptophan hydroxylase as novel target for the treatment of depressive disorders. *Pharmacology* 85(2), 95–109 (2010).
14. Patrick RP, Ames BN. Vitamin D hormone regulates serotonin synthesis. Part 1: relevance for autism. *FASEB J.* 28(6), 2398–2413 (2014).
15. Eissa N, Al-Houqani M, Sadeq A, Ojha SK, Sasse A, Sadek B. Current enlightenment about etiology and pharmacological treatment of autism spectrum disorder. *Front. Neurosci.* 12, 304 (2018).
16. Fitzpatrick PF, Ralph EC, Ellis HR, Willmon OJ, Daubner SC. Characterization of metal ligand mutants of tyrosine hydroxylase: insights into the plasticity of a 2-histidine-1-carboxylate triad. *Biochemistry* 42(7), 2081–2088 (2003).

17. Abu-Omar MM, Loaiza A, Hontzeas N. Reaction mechanisms of mononuclear non-heme iron oxygenases. *Chem. Rev.* 105(6), 2227–2252 (2005).
18. Walther DJ, Bader M. A unique central tryptophan hydroxylase isoform. *Biochem. Pharmacol.* 66(9), 1673–1680 (2003).
19. Walther DJ, Peter JU, Bashammakh S *et al.* Synthesis of serotonin by a second tryptophan hydroxylase isoform. *Science* 299(5603), 76 (2003).
20. McKinney J, Knappskog PM, Haavik J. Different properties of the central and peripheral forms of human tryptophan hydroxylase. *J. Neurochem.* 92(2), 311–320 (2005).
21. Amireault P, Sibon D, Cote F. Life without peripheral serotonin: insights from tryptophan hydroxylase 1 knockout mice reveal the existence of paracrine/autocrine serotonergic networks. *ACS Chem. Neurosci.* 4(1), 64–71 (2013).
22. Cote F, Thevenot E, Fligny C *et al.* Disruption of the nonneuronal *TPH1* gene demonstrates the importance of peripheral serotonin in cardiac function. *Proc. Natl Acad. Sci. USA* 100(23), 13525–13530 (2003).
23. Malek ZS, Dardente H, Pevet P, Raison S. Tissue-specific expression of tryptophan hydroxylase mRNAs in the rat midbrain: anatomical evidence and daily profiles. *Eur. J. Neurosci.* 22(4), 895–901 (2005).
24. Gutknecht L, Waider J, Kraft S *et al.* Deficiency of brain 5-HT synthesis but serotonergic neuron formation in TPH2 knockout mice. *J. Neural Transm. (Vienna)* 115(8), 1127–1132 (2008).
25. Waloen K, Kleppe R, Martinez A, Haavik J. Tyrosine and tryptophan hydroxylases as therapeutic targets in human disease. *Expert Opin. Ther. Targets* 21(2), 167–180 (2017).
26. Bader M. Inhibition of serotonin synthesis: a novel therapeutic paradigm. *Pharmacol. Ther.* 205, 107423 (2020).
27. Engelman K, Lovenberg W, Sjoerdsma A. Inhibition of serotonin synthesis by para-chlorophenylalanine in patients with the carcinoid syndrome. *N. Engl. J. Med.* 277(21), 1103–1108 (1967).
28. Zimmer L, Luxen A, Giacomelli F, Pujol JF. Short- and long-term effects of p-ethynylphenylalanine on brain serotonin levels. *Neurochem. Res.* 27(4), 269–275 (2002).
29. Cianchetta G, Stouch T, Yu W *et al.* Mechanism of inhibition of novel tryptophan hydroxylase inhibitors revealed by co-crystal structures and kinetic analysis. *Curr. Chem. Genomics* 4, 19–26 (2010).
30. Goldberg DR, De Lombaert S, Aiello R *et al.* Optimization of spirocyclic proline tryptophan hydroxylase-1 inhibitors. *Bioorg. Med. Chem. Lett.* 27(3), 413–419 (2017).
31. Markham A. Telotristat ethyl: first global approval. *Drugs* 77(7), 793–798 (2017).
32. Masab M, Saif MW. Telotristat ethyl: proof of principle and the first oral agent in the management of well-differentiated metastatic neuroendocrine tumor and carcinoid syndrome diarrhea. *Cancer Chemother. Pharmacol.* 80(6), 1055–1062 (2017).
33. Liu Q, Yang Q, Sun W *et al.* Discovery and characterization of novel tryptophan hydroxylase inhibitors that selectively inhibit serotonin synthesis in the gastrointestinal tract. *J. Pharmacol. Exp. Ther.* 325(1), 47–55 (2008).
34. Shi H, Cui Y, Qin Y. Discovery and characterization of a novel tryptophan hydroxylase 1 inhibitor as a prodrug. *Chem. Biol. Drug Des.* 91(1), 202–212 (2018).
35. Petrassi M, Barber R, Be C *et al.* Identification of a novel allosteric inhibitory site on tryptophan hydroxylase 1 enabling unprecedented selectivity over all related hydroxylases. *Front. Pharmacol.* 8, 240 (2017).
36. Teigen K, McKinney JA, Haavik J, Martinez A. Selectivity and affinity determinants for ligand binding to the aromatic amino acid hydroxylases. *Curr. Med. Chem.* 14(4), 455–467 (2007).
37. Lo MC, Aulabaugh A, Jin G *et al.* Evaluation of fluorescence-based thermal shift assays for hit identification in drug discovery. *Anal. Biochem.* 332(1), 153–159 (2004).
38. Niesen FH, Berglund H, Vedadi M. The use of differential scanning fluorimetry to detect ligand interactions that promote protein stability. *Nat. Protoc.* 2(9), 2212–2221 (2007).
39. Wang L, Erlandsen H, Haavik J, Knappskog PM, Stevens RC. Three-dimensional structure of human tryptophan hydroxylase and its implications for the biosynthesis of the neurotransmitters serotonin and melatonin. *Biochemistry* 41(42), 12569–12574 (2002).
40. McKinney J, Knappskog PM, Pereira J *et al.* Expression and purification of human tryptophan hydroxylase from *Escherichia coli* and *Pichia pastoris*. *Protein Expr. Purif.* 33(2), 185–194 (2004).
41. Winge I, McKinney JA, Knappskog PM, Haavik J. Characterization of wild-type and mutant forms of human tryptophan hydroxylase 2. *J. Neurochem.* 100(6), 1648–1657 (2007).
42. Flydal MI, Chatfield CH, Zheng H *et al.* Phenylalanine hydroxylase from *Legionella pneumophila* is a thermostable enzyme with a major functional role in pyomelanin synthesis. *PLoS ONE* 7(9), e46209 (2012).
43. Aubi O, Flydal MI, Zheng H *et al.* Discovery of a specific inhibitor of pyomelanin synthesis in *Legionella pneumophila*. *J. Med. Chem.* 58(21), 8402–8412 (2015).
44. Haavik J, Flatmark T. Rapid and sensitive assay of tyrosine 3-monooxygenase activity by high-performance liquid chromatography using the native fluorescence of DOPA. *J. Chromatogr.* 198(4), 511–515 (1980).

45. Szigetvari PD, Muruganandam G, Kallio JP *et al.* The quaternary structure of human tyrosine hydroxylase: effects of dystonia-associated missense variants on oligomeric state and enzyme activity. *J. Neurochem.* 148(2), 291–306 (2019).
46. Friesner RA, Murphy RB, Repasky MP *et al.* Extra precision glide: docking and scoring incorporating a model of hydrophobic enclosure for protein-ligand complexes. *J. Med. Chem.* 49(21), 6177–6196 (2006).
47. Dai R, Geders TW, Liu F *et al.* Fragment-based exploration of binding site flexibility in Mycobacterium tuberculosis BioA. *J. Med. Chem.* 58(13), 5208–5217 (2015).
48. Morreale FE, Bortoluzzi A, Chaugule VK, Arkinson C, Walden H, Ciulli A. Allosteric targeting of the Fanconi anemia ubiquitin-conjugating enzyme Ube2T by fragment screening. *J. Med. Chem.* 60(9), 4093–4098 (2017).
49. Sayegh J, Cao J, Zou MR *et al.* Identification of small molecule inhibitors of Jumonji AT-rich interactive domain 1B (JARID1B) histone demethylase by a sensitive high throughput screen. *J. Biol. Chem.* 288(13), 9408–9417 (2013).
50. Calvo AC, Scherer T, Pey AL *et al.* Effect of pharmacological chaperones on brain tyrosine hydroxylase and tryptophan hydroxylase 2. *J. Neurochem.* 114(3), 853–863 (2010).
51. Thony B, Calvo AC, Scherer T *et al.* Tetrahydrobiopterin shows chaperone activity for tyrosine hydroxylase. *J. Neurochem.* 106(2), 672–681 (2008).
52. Frantom PA, Seravalli J, Ragsdale SW, Fitzpatrick PF. Reduction and oxidation of the active site iron in tyrosine hydroxylase: kinetics and specificity. *Biochemistry* 45(7), 2372–2379 (2006).
53. Renson J, Weissbach H, Udenfriend S. Hydroxylation of tryptophan by phenylalanine hydroxylase. *J. Biol. Chem.* 237, 2261–2264 (1962).
54. Jin H, Cianchetta G, Devasagayaraj A *et al.* Substituted 3-(4-(1,3,5-triazin-2-yl)-phenyl)-2-aminopropanoic acids as novel tryptophan hydroxylase inhibitors. *Bioorg. Med. Chem. Lett.* 19(17), 5229–5232 (2009).
55. Shi ZC, Devasagayaraj A, Gu K *et al.* Modulation of peripheral serotonin levels by novel tryptophan hydroxylase inhibitors for the potential treatment of functional gastrointestinal disorders. *J. Med. Chem.* 51(13), 3684–3687 (2008).
56. Ouyang L, He G, Huang W, Song X, Wu F, Xiang M. Combined structure-based pharmacophore and 3D-QSAR studies on phenylalanine series compounds as TPH1 inhibitors. *Int. J. Mol. Sci.* 13(5), 5348–5363 (2012).